Investigating the influence of a thin copper film coated on nickel plates through physical vapor deposition for electrocatalytic nitrate reduction

Meshram, Sumit Maya Moreshwar; Gonugunta, Prasad; Taheri, Peyman; Jourdin, Ludovic; Pande, Saket

DOI
10.3389/fmats.2025.1527753

Publication date
2025

Document Version
Final published version

Published in
Frontiers in Materials

frontiers | Frontiers in Materials

TYPE Original Research
PUBLISHED 26 May 2025
DOI 10.3389/fmats.2025.1527753

OPEN ACCESS

EDITED BY
Ahmed Eid Hassan,
Al-Azhar University, Egypt

REVIEWED BY
Manisha Das,
Japan Society for the Promotion of Science (JSPS), Japan
Dipayan Pal,
University of California, San Diego, United States

*CORRESPONDENCE
Sumit Maya Moreshwar Meshram,
s.m.meshram@tudelft.nl

RECEIVED 13 November 2024
ACCEPTED 21 April 2025
PUBLISHED 26 May 2025

CITATION
Meshram SMM, Gonugunta P, Taheri P, Jourdin L and Pande S (2025) Investigating the influence of a thin copper film coated on nickel plates through physical vapor deposition for electrocatalytic nitrate reduction.
Front. Mater. 12:1527753.
doi: 10.3389/fmats.2025.1527753

Investigating the influence of a thin copper film coated on nickel plates through physical vapor deposition for electrocatalytic nitrate reduction

Sumit Maya Moreshwar Meshram[1]*, Prasad Gonugunta[2], Peyman Taheri[2], Ludovic Jourdin[3] and Saket Pande[1]

[1]Department of Water Management, Faculty of Civil Engineering and Geosciences, Delft University of Technology, Delft, Netherlands, [2]Department of Materials Science and Engineering (MSE), Faculty of Mechanical Engineering, Delft University of Technology, Delft, Netherlands, [3]Department of Biotechnology, Faculty of Applied Sciences, Delft University of Technology, Delft, Netherlands

The removal of nitrate (NO_3^-) from water and its subsequent valorization for various applications are crucial due to environmental, health, and economic considerations. A promising method for its removal is the process of electrocatalytic reduction of nitrate. Copper/nickel (Cu/Ni) composite electrodes have demonstrated potential for this process in aqueous solution, however, the effect of thin Cu film coated on Ni using physical vapor deposition (PVD) has not been investigated for NO_3^- removal. Here, the PVD technique was employed to deposit a thin film of Cu onto a Ni plate to form Cu-Ni composite electrodes of varying Cu thicknesses (25–100 nm), enabling the investigation of the influence of the Cu film thickness on NO_3^- reduction. Electrodes prepared using PVD were utilized for electrocatalytic nitrate reduction (NO_3RR) for the first time. The Cu-Ni electrodes were analyzed using X-ray photoelectron spectroscopy (XPS) and scanning electron microscopy (SEM) to examine the deposited Cu film which is critical for NO_3^- reduction and ammonium (NH_4^+) selectivity. The Cu film was found to be uniformly distributed on the Ni plate without any additional contamination. Cyclic voltammetry was performed to obtain the information on electron transfer between the Cu-Ni electrode and the nitrogen (N_2) species on the surface. NO_3^- was primarily reduced to NH_4^+, with no significant difference in the NO_3^- conversion rate observed as a function of the Cu thickness. As the Cu thickness increased, the current density decreased. This study also investigated the effect of stirring on NO_3^- reduction, considering potential applications where rotation or stirring is not feasible such as in some batteries. The findings of this investigation indicate that thin film coated electrodes fabricated using the PVD method exhibit capability for NO_3^- elimination through electrocatalytic reduction processes.

KEYWORDS

physical vapor deposition, electrocatalytic nitrate reduction, copper-nickel electrode, thickness, XPS, SEM

1 Introduction

Nitrate (NO_3^-) is one of the most common toxic pollutants in groundwater (Li et al., 2015). NO_3^- contamination of groundwater is becoming increasingly serious in both developed and developing countries (Sancho et al., 2016; Jia et al., 2020; Abba et al., 2023). This problem is caused by a variety of activities, including agriculture, industry, sewage, septic tanks, and landfills, leading to an increase in NO_3^- levels in water sources (Lockhart et al., 2013; Abascal et al., 2022). The maximum amount of NO_3^- permitted in drinking water is 50 mg/L in Europe and 44.43 mg/L in the United States (Shen et al., 2009). Methemoglobinemia or "blue baby syndrome" can result from NO_3^- exposure above these levels and poses substantial health hazards, especially for young children and expectant mothers (Knobeloch et al., 2000). Additionally, NO_3^- poisoning of water, used for agriculture has an impact on both ecosystems and human health (Della Rocca et al., 2007). Water bodies are also affected by excessive NO_3^- contamination, resulting in eutrophication, algal blooms, and disruption of the delicate balance of aquatic life (Moffat, 1998). Thus, to maintain the water quality, public health, and ecological integrity of agricultural watersheds, effective NO_3^- removal technologies are essential (Tomer et al., 2013).

Various methods have been developed to remove NO_3^- from water, including reverse osmosis (Ahn et al., 2008), ion exchange (Leaković et al., 2000), electrodialysis (El Midaoui et al., 2002), photocatalytic reduction (Varapragasam et al., 2021), and biological denitrification (Park and Yoo, 2009). In recent times, electrochemical methods, particularly electrocatalytic nitrate reduction (NO_3RR), have gained recognition as a viable solution for the efficient elimination of low-concentration NO_3^- from water sources (de Groot and Koper, 2004). Although, still it is in the developmental stage, this technology holds immense promise. When it is fully realized, it can offer numerous advantages over conventional approaches, including environmental sustainability, compatibility, cost-effective energy consumption, high efficiency, satisfactory engineering compatibility, controllable operating conditions, selectivity to desired product, and potential integration with renewable energy sources (Lange et al., 2013; Jia et al., 2020; Wang Y. et al., 2021). Two routes are involved in the NO_3RR (Wang H. et al., 2023): The indirect autocatalytic reduction pathway and the direct electrocatalytic reduction pathway. Indirect autocatalytic reduction occurs when NO_3^- is not involved in electron transfer processes (de Groot and Koper, 2004; Wang Y. et al., 2021). This indirect autocatalytic reduction pathway usually occurs only at high NO_3^- concentrations and in strongly acidic media (Lange et al., 2013). Direct reductive chemical pathways are possible at low concentrations of NO_3^-. In the NO_3^- reduction process, nitrogen (N_2) and ammonia (NH_3) are the main products, following reactions (Equations 1–5):

$$NO_3^- + H_2O + 2e^- \rightarrow NO_2^- + 2OH^- \quad (1)$$

$$NO_2^- + 2H_2O + 3e^- \rightarrow \frac{1}{2}N_2 + 4OH^- \quad (2)$$

$$NO_2^- + 5H_2O + 6e^- \rightarrow \frac{1}{2}NH_3 + 7OH^- \quad (3)$$

$$NO_2^- + 4H_2O + 6e^- \rightarrow NH_2OH + 5OH^- \quad (4)$$

$$NO_2^- + H_2O + 2e^- \rightarrow NO + 2OH^- \quad (5)$$

From the Pourbaix diagram shown in Figure 1, N_2 and NH_3 are the most thermodynamically stable forms of N_2 under standard conditions (Guo et al., 2019).

NO_3^- is more stable in alkaline solution. In alkaline solution, the reduction of NO_3^- will yield a series of products (e.g., dinitrogen tetraoxide (N_2O_4), hydrazine (N_2H_4), nitric oxide (NO), and hydroxylamine (NH_2OH)) which are not the primary products in NO_3^- reduction and may decompose into other species. The existing form of ammonia (NH_3) depends on the pH of the solution, where at pH ≥ 9.25, it exists in its molecular form, and at pH < 9.25, ionic NH_4^+ is the major form. For N_2H_4, the case is similar, where the pH boundary is 6.07.

NO_3RR process involves the use of electrocatalysts, such as non-noble metals (e.g., Cu, Ni, Co, and Fe) or carbon-based materials, to reduce NO_3^- to N_2 gas or NH_3 (Liang et al., 2022; Zhang et al., 2022). The choice of electrocatalyst affects the reaction kinetics, selectivity, and efficiency (Xu et al., 2023). Copper (Cu) and Cu-based materials are considered the most promising (Hu et al., 2021; He L. et al., 2022) because of their low cost, abundant availability (Feng et al., 2022), high activity (Hu et al., 2021; Hong et al., 2022; Barrera et al., 2023), and excellent performance in producing NH_3 as the main electrolysis product (Abdallah et al., 2014; Wang et al., 2020; Karamad et al., 2023; Li X. et al., 2023). Cu is an active monometallic electrocatalyst for the NO_3RR in acidic and alkaline electrolytes. It also exhibit good electrocatalytic activity in both acidic and alkaline media (Hasnat et al., 2015).

NO_3^- reduction on Cu is a pH-dependent reaction forming NO and NH_4^+ when an acidic electrolyte is used and NO_2^- and NH_2OH when the electrolyte is alkaline (Pérez-Gallent et al., 2017). Metallic Cu effectively attracts and retains oxygen (O) atoms from NO_3^-. This interaction weakens the N-O bonds in NO_3^-, creating a low energy point in the bond's profile. Consequently, this facilitates the conversion of NO_3^- into nitrite (NO_2^-) by easing the detachment of one oxygen atom from N_2 (Liu et al., 2019). In the process of NO_3^- reduction, the movement of charge is typically slow due to the high energy present in the lowest unoccupied π molecular (LUMO) orbital of NO_3^-. This makes it difficult to inject charge into this orbital. However, the d-orbital energy levels of Cu-based materials are similar to the LUMO*of NO_3^- (Hao et al., 2021) allowing them to facilitate the electrochemical reduction of NO_3^-(aq) and transfer electrons more easily to the adsorbed NO_3^- (Reyter, 2014; Rezaei-Sameti and Zarei, 2018; Beltrame et al., 2021a; Wei M. et al., 2024). Various studies have shown that Cu electrodes are used for NO_3^- reduction in a single chamber in acidic (Burke and Sharna, 2007; Lima et al., 2012), in neutral (Gao et al., 2018), and in alkaline media (Paidar et al., 1999; Bouzek et al., 2001; Badea, 2009), as well as in dual chambers in acidic (Beltrame et al., 2021b), and alkaline media (Cattarin, 1992; Badea, 2009; Rajmohan and Chetty, 2014). In alkaline media, Cu electrodes produce fewer oxides of N_2 as byproducts, and are less corrosive than in acidic media (Badea, 2009). However, despite its advantages, there are some disadvantages with pure Cu catalysts, such as oxidative dissolution or irreversible surface poisoning, both of which lead to undesired catalyst degradation (Dima et al., 2003;

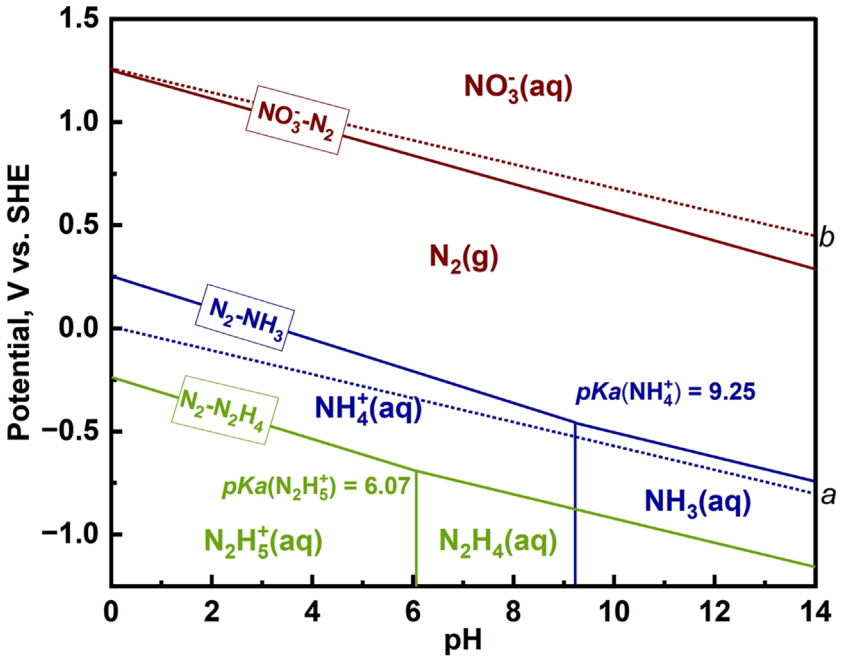

FIGURE 1
Pourbaix diagram of the N_2-H_2O system including N_2, NH_3, N_2H_4, and NO_3^-.

Hou et al., 2018), as well as undesirable formation of unwanted by-products (Reyter et al., 2006; Abdallah et al., 2014), such as NO_2^- (Roy et al., 2016; He W. et al., 2022).

To overcome the disadvantages of Cu electrodes, various strategies have been developed including (i) engineering Cu into nanoscale or single reaction site (Zhao et al., 2023), (ii) doping Cu with other elements (Pd, P, Ni, etc.), and (iii) depositing Cu on a metal oxide support (Liu Z. et al., 2023). Depositing Cu on a metal oxide support is the most preferred strategy, as it is simple to synthesize and provides considerable benefits from strong metal-support interactions (Smiljanić et al., 2022). There are various thin surface film deposition techniques (Jilani et al., 2017; Abegunde et al., 2019) for depositing or coating Cu such as electrochemical deposition (Epron et al., 2001; Epron et al., 2002; Ramos et al., 2001; Welch et al., 2005; Molodkina et al., 2010; Couto et al., 2011; Couto et al., 2017; Chen and Chang, 2012; Liu and Zou, 2014; Rajmohan and Chetty, 2014; Alam et al., 2015; Mattarozzi et al., 2017; Hou et al., 2018; Lei et al., 2018; Gao et al., 2019; Yin et al., 2019; Zhao et al., 2022; Zurita and Garcia, 2022; Wang C. et al., 2023; Zurita and García, 2023), photo-electrodeposition (Couto et al., 2012; Ribeiro et al., 2014), potentiostatic deposition (Roy et al., 2016; Chen et al., 2023; Lim et al., 2023), electro-crystallization (Hyusein and Tsakova, 2023) and dipping method (Hwang, 2012).

Using the above deposition techniques Cu has been deposited on many substrates such as palladium (Lim et al., 2023), graphene oxide (GO), modified graphite felt (Wang et al., 2022), polydopamine-derived nitrogen-doped hollow carbon spheres (Liu Y. et al., 2023), carbon nanotubes (Rajmohan and Chetty, 2017), Cu foil (Rajmohan and Chetty, 2014), and zinc oxide (Feng et al., 2024). Nickel (Ni) is also utilized as a substrate for catalyst preparation but mostly by forming an alloy with Cu. This approach is employed because Ni produces a homogeneous, stable, and highly active catalyst with Cu, exhibiting high chemical stability and good electron conductivity (Hou et al., 2018). Additionally, its site demonstrates strong adsorption for NO_2^- (He L. et al., 2022). The combination of Cu and Ni compensates for the low activity of pure Cu in mediating electron transfer between intermediates (Kobune et al., 2020; Shih et al., 2020; Bai et al., 2023), and reduces the overpotential while improving the stability of the NO_3RR reaction (Bai et al., 2023). However, Cu deposition on Ni using electrochemical deposition, results in uneven film thicknesses due to variation in applied current densities (Goranova et al., 2016), electrolyte composition (Dejang et al., 2025), and temperature (Abdullah, 2017).

The film thickness and electrolyte concentration govern NO_3RR activity (Roy et al., 2016; Guo et al., 2023). The thickness of Cu film affects the activity and selectivity for NO_3^- reduction (Chen et al., 2004; Shih et al., 2020). So, here PVD technique is adopted as it can provide coatings with high precision for various film thicknesses. In addition, PVD has several advantages over other coating techniques, such as high-purity coatings (Takahashi, 1998; Yanguas-Gil and Yanguas-Gil, 2017), low processing temperature (Shah et al., 2018), high deposition rates, better adhesion, denser microstructure, controllable material properties, the ability to use a larger choice of materials (Savale, 2016; Morgan et al., 2019), reduced production cost, improved productivity (Mubarak et al., 2005), and better quality films (O'Sullivan et al., 2002). Table 1 presents the state-of-the-art techniques for electrode preparation utilized in NO_3^- reduction, delineating the chemicals employed, electrolyte used, duration, and efficacy in NO_3^- reduction. It is significant to note that all previous investigations exclusively utilized Ni foam, with no studies exploring Ni plate as an alternative substrate for

TABLE 1 State-of-the-art electrode preparation techniques utilized for nitrate reduction employing Cu coated on Ni.

Sr.No	Electrode	Electrode preparation technique	Chemical composition	Electrolyte	Duration (hour)	Nitrate reduction efficiency	References
1	NiCu@N-C/Ni Foam	Co-assembly and carbothermic reduction	3.57 mM NO_3^-	50 mM SO_4^{2-}	8	98.63%	He et al. (2022a)
2	$Cu_{0.66}Ni_{0.33}$ $Cu_{0.50}Ni_{0.50}$ $Cu_{0.33}Ni_{0.66}$	Electrodeposition	0.01 mol/L $NaNO_3$	0.1 mol/L Na_2SO_4	4	83.87%	Bai et al. (2023)
3	Cu – Ni Foam	Cold plasma jet printing	50 mg/L $NaNO_3$	0.05 mol Na_2SO_4	3	88.9%	Yue et al. (2024)
4	Cu_3P-Ni_2P/CP-x	Vapor-phase hydrothermal method	200 ppm $NaNO_3$-N	0.5 M Na_2SO_4	2	—	Jin et al. (2024)
5	Cu and NiO rod on Ni foam	Electrodeposition	0.1M KNO_3-N	0.1M PBS	1	94%	Liu et al. (2023a)
6	Cu/CoP/Ni Foam	Hydrothermal	15 mg/L NO_3-N	0.05 M Na_2SO_4 and 0–2000 mg/L Cl^-	3.5	100%	Yang et al. (2022)
7	Cu on Ni Foam	Electrodeposition	200 ppm NO_3-N	1M KOH	2	95.05%	Li et al. (2021)
8	CuNi alloy on mesoporous carbon	Evaporation-induced self-assembly	30 mg/L NO_3^--N	0.1M Na_2SO_4	7	90%	Yao et al. (2021)
9	$Cu(OH)_2$-Cu/NiFoam	One-step hydrothermal method	50 mg/L NO_3^--N	50 mM Na_2SO_4	1.5	91.5%	Liang et al. (2023)
10	Cu nanoparticles on Ni plate	Physical vapour deposition	2.5 mM KNO_3	0.5 g/L of Na_2SO_4	6	10%	This study

NO_3^- reduction. The Ni plate is chosen over Ni foam because it provides a more robust and stable structure compared to Ni foam, which helps maintain the catalyst's integrity during prolonged electrochemical operations. This enhanced stability reduces the likelihood of structural breakdown often seen in the more fragile foam configuration (Kabiraz et al., 2024). Also, when Cu is deposited on Ni using electrochemical deposition, it shows poor stability owing to the oxidation and detachment of the deposited Cu layer from the substrates during the course of NO_3^- electroreduction (Hou et al., 2018). Furthermore, Ni foam is prone to corrosion, resulting in the release of free Ni ions. This process alters the catalyst's composition and hinders the subsequent analysis of related catalytic mechanisms (Bu et al., 2021). Moreover, the utilization of PVD for electrode preparation has not been previously investigated in this field of research, as noted in (Yue et al., 2024).

Therefore the primary objective of this research is to investigate the influence of thin Cu film coated on Ni plate using PVD technique for NO_3RR. Previous investigations that employed Cu coating for electrode preparation have deposited thin Cu films varying from 1 nm to 390 nm on various substrates that were used as electrodes for diverse applications except NO_3^- reduction (Raaif and Mohamed, 2017; Gonzalez-Gallardo et al., 2024; Johnston et al., 2004; Löffler and Siewert, 2004; Nobili et al., 2009; Wu et al., 2010; Ince et al., 2012; Kang et al., 2013; Salazar et al., 2015; 2016; Sun et al., 2015; Ganchev et al., 2021). Therefore, in this study thicknesses of 25, 50, and 100 nm were selected to encompass this range. Subsequently, the effect of Cu film on the NO_3RR was examined. Additionally, the effect of stirring on the NO_3^- reduction reaction was investigated. Further, the obtained Cu-Ni electrodes were analyzed using scanning electron microscopy (SEM) and X-ray photoelectron spectroscopy (XPS).

2 Experimental methods

2.1 Chemicals and materials

All chemicals used in this study were of analytical grade and purchased from Sigma Aldrich. Potassium nitrate (KNO_3) and sodium sulphate (Na_2SO_4) were used to prepare the anolyte and catholyte. Pure Cu powder with a particle size <425 μm, density of Cu = 8.930, Z-ratio = 0.437, and 99.5% purity was utilized for the deposition on Ni plates. These Ni plates served as substrates for the Cu films coating, which functioned as the cathodes in subsequent analysis. The Ni plates (purity = 99.96%, thickness = 0.2 mm) were purchased from Haoxuan Metal Materials Ltd.

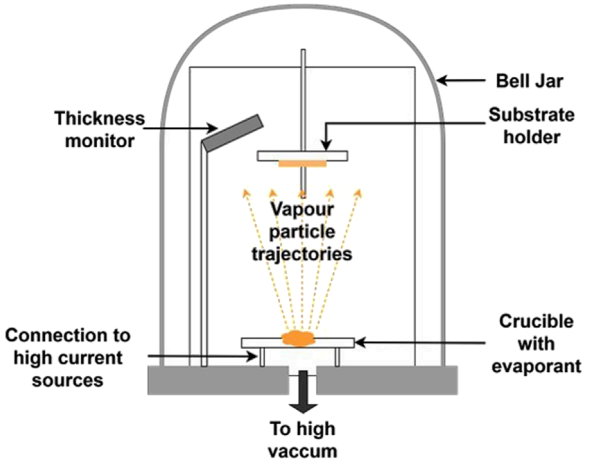

FIGURE 2
Schematic of the PVD equipment and Cu deposition process on a Ni plate.

Platinum mesh was used as anode. All solutions were prepared using milliQ water (water obtained from a Millipore system). pH of the solution was measured using a Multi9420 InoLab IDS multimeter. Spectrophotometer (model number: DR3900) was employed for determining the concentration of NO_3^-, NO_2^-, and NH_4^+. The LCK 340, LCK 342, and LCK (303 and304) Hach kits were utilized for measuring NO_3^-, NO_2^-, and NH_4^+, respectively.

2.2 Synthesis of thin films of Cu on Ni plate using physical vapor deposition

First, the Ni plate was sanded and polished with sandpaper of grit size 400–2000. To remove impurities, the Ni sheet (of purity >99.8%) was ultrasonically degreased and cleaned in acetone and ethanol for 15 min. They were then immersed in a 1 mol.L^{-1} aqueous hydrochloric acid (HCl) solution for 5 min and washed with milliQ water. 25, 50, and 100 nm thickness of the Cu was deposited on both sides of Ni plate using the PVD (VCM 600-SP3, rack-type vacuum evaporator) method by applying a current of ~80 A. The operation details of the PVD are: substrate temperature = 1,600–1,800°C, evaporation rate = 0.5 Å/s, current intensity = 150 Amp, base pressure = 2.8×10^{-7} mbar, and vacuum of 5.0×10^{-6} mbar was achieved. The PVD involves the condensation of vaporized Cu atoms onto a Ni substrate under vacuum conditions, resulting in the formation of a uniform and cohesive layer (Rossnagel, 2003). The Cu–Ni sheet of 2 cm × 1 cm was dried in air at room temperature. Figure 2 shows a schematic of the PVD equipment and the synthesis of Cu-Ni electrodes.

2.3 Electrochemical NO_3^- reduction

The NO_3^- electrochemical reduction experiments were carried out using a three-electrode system in a 300 mL dual-chamber H-type reactor, as shown in Supplementary Figure S1 [Supplementary Material (SI)]. The anolyte was 3.5 mM Na_2SO_4, whereas the catholyte consisted of 2.5 mM KNO_3 and 0.5 g/L of Na_2SO_4 solution. 300 mL of catholyte was placed in the cathode chamber, which was then sparged with N_2 gas to remove oxygen from the solution to create anaerobic conditions. A Pt mesh (1 cm × 1 cm) was used as the counter (anode) electrode. A Cu-Ni plate (2 cm × 1 cm) was cut from a large Cu-Ni plate and used as the working electrode (cathode). The surface area of the working electrode was 4 cm^2. Ag/AgCl (3 M KCl) was used as the reference electrode. A titanium wire was connected to the Cu-Ni plate to form an external connection with the potentiostat (Admiral instrument's Squidstat Prime). A proton exchange membrane (Nafion 117) was used to separate anode and cathode chambers. A gas bag was attached to the anode and cathode chamber to collect any produced gases like H_2. All electrochemical experiments were performed by applying a constant current of −8.5 mA for 6 h. Approximately 10 mL of the solution was removed between two sampling points to determine the concentrations of NO_3^-, NO_2^-, and NH_4^+ ions and was replaced with fresh catholyte solution. NO_3^-, NO_2^-, and NH_4^+ in the solutions were measured using standard Hach kits with a UV-visible spectrophotometer (DR-3900, Lange). Cyclic voltammetry (CV) was performed at a potential scan rate of 1 mV/s under two conditions: with stirring at 500 rotation per minute (rpm) and without stirring.

The conversion rate [C (NO_3^-)%] of NO_3^- was calculated using Equation 6

$$C[NO_3^-]\% = \frac{C_0[NO_3^- - N] - C_t[NO_3^- - N]}{C_0[NO_3^- - N]} \times 100\% \quad (6)$$

The selectivity [S (NH_4^+)%] of NH_4^+ can be calculated based on Equation 7

$$S[NH_4^-]\% = \frac{C_t[NH_4^- - N]}{C_0[NO_3^- - N] - C_t[NO_3^- - N]} \times 100\% \quad (7)$$

The concentration of gaseous compounds was calculated using mass balance Equation 8

$$C\,[Gaseous\ compounds] = \{C_0[NO_3^- - N] - \left(C_{nitrate\ remaining\ in\ solution} + C_{nitrite} + C_{ammonium}\right)\} \quad (8)$$

where, $C_0(NO_3^- - N)$ is initial the concentration of NO_3^- – N (mg/l), V is the volume of the electrolyte in the cathode compartment (L), where subscript '0' represents the initial condition whereas 't' represents the condition after time 't'.

2.4 Electrode surface characterization

The morphologies of the samples were examined using field-emission scanning electron microscope (FE-SEM, JEOL JSM 6500F), which was equipped with an EDX detector. The surface chemistry of the samples was analyzed using a PHI-TFA XPS spectrometer from Physical Electronic Inc., which featured an Al Kα X-ray monochromatic source (hv = 1486.7 eV). The pass energy for the survey was set at 89.45 eV, and a vacuum of approximately 10^{-9} mbar was maintained during the XPS analysis (Cornet et al., 2024). Data was analyzed using Multipak version 8.0 software.

3 Results and discussions

3.1 Characterization

Supplementary Figure S2 showcases SEM images of Cu-Ni electrodes, which were fabricated through PVD for the 25 nm thickness at 370x (Supplementary Figure S2A), and 4,000x (Supplementary Figure S2B) magnifications. Supplementary Figure S3 shows the elemental EDX mapping and spectrum of 25 nm Cu-Ni electrode. The elemental EDX mapping of pristine Cu-Ni electrode demonstrates the complete coverage of the Ni plate with Cu, a finding that is consistent with the XPS results.

Supplementary Figures S4–S6 (shown in SI) depict the XPS of Ni plate, Cu-Ni electrode with 25 nm Cu coating (pristine) and (spent) after electrochemical reduction of NO_3^-, respectively. The detailed explanation about the XPS analysis given in SI. Supplementary Figure S7 depicts a comparison of XPS spectra of Ni 2p of Ni plate without coating (Supplementary Figure S7A), 25 nm Cu-Ni electrode (pristine) (Supplementary Figure S7B), and 25 nm Cu-Ni electrode (spent) (Supplementary Figure S7C). A noticeable difference in peaks can be observed for all three electrodes. The Ni plate without a coating exhibits the highest peaks, corresponding to Ni^0, Ni^{2+}, and Ni^{3+}, whereas no peaks were detected for the Cu-Ni electrode (pristine). For the Cu-Ni electrode (spent), Ni peaks are barely visible, indicating that some Cu has been removed, exposing the Ni surface during NO_3RR facilitating the NO_3^- reduction. A schematic diagram depicting the mechanism of Cu removal from the cathode during NO_3^- reduction is illustrated in Supplementary Figure S8.

3.2 Electrochemical measurements

3.2.1 Cyclic voltammetry (CV) in H-type reactor

To assess the electrocatalytic performance of Cu deposition of different thicknesses on Ni plates, CV experiments were conducted. Figure 3 depicts the CV curves obtained for various concentrations of KNO_3 and Na_2SO_4 electrolyte solutions in the range of −1.8 to −0.4 V (versus Ag/AgCl (3 M KCl) reference electrode) at a scan rate of 1 mV/s.

From the cyclic voltammograms (CVs) shown in Figure 3, an onset potential at ca. −0.603 ± 0.015 V (black curve), −0.617 ± 0.015 V (green curve), and −0.687 ± 0.031 V (red curve) was clearly visible for the experiments in which KNO_3 + Na_2SO_4 was fed and stirring was absent. No visible peak corresponding to NO_3^- reduction was detected under stirred conditions. The absence of a NO_3RR peak was anticipated, as mass transport is not limited under stirring which facilitates faster replenishment of NO_3^- at the cathode surface than it is consumed, and products are also removed faster from the surface. This is in contrast to the situation when stirring is ceased, resulting in the formation of a peak, in the −0.6 to −1 V range with a maximum at around −0.9 V vs. Ag/AgCl (where no or limited H_2 production was observed). For 5.9 mM KNO_3 + 3.5 mM Na_2SO_4, concentration in stirring conditions (red curves) the potential of the reductive peak shifted to slightly more negative potentials, ca. −1.03 ± 0.15 V vs Ag/AgCl. For the experiments that contained only for 3.5 mM Na_2SO_4 (pink curves), no peak was observed, and an onset in reductive current was only observed at ca. −0.85 ± 0.03 V (with stirring) and −0.88 ± 0.01 V (without stirring), is either corresponds to proton (H^+) and/or water reduction to H_2. The current densities at the NO_3RR peak in without stirring condition were ca. 1.48 ± 0.59 (black curve), 1.36 ± 0.68 (green curve), and 2.33 ± 0.11 mA cm^{-2} (red curve). Therefore, the presence of 5.9 mM KNO_3 (red curves) partially alleviated mass transport limitations (without stirring), resulting in a higher NO_3RR peak compared to 2.5 mM KNO_3 (black curves). No significant differences in peak height and onset were observed at varying Cu layer thicknesses without stirring, except for a slightly higher maximum peak current at 5.9 mM KNO_3 (red curve) and 100 nm Cu film thickness. With 25 and 100 nm thick Cu film and under stirring, a higher reductive current was recorded with 5.9 mM KNO_3 than with 2.5 mM KNO_3 in the −0.6 to −1 V range, which would indicate a higher rate of NO_3^- reduction, though this was not observed for 50 nm Cu film. As the Cu film thickness on the Ni plate is enhanced, a decrease in the current density is observed, as illustrated in Supplementary Figure S9. This could be due to the evolution of microstructure and increased surface roughness (Lin et al., 2017), structural deterioration (Nguyen et al., 2024), and increased resistivity caused by variations in bonding mechanisms and interface voids in thicker films which impedes current flow (Lu T.-F. et al., 2024). Further investigation is necessary to elucidate these observations.

3.3 NO_3RR using 25 nm, 50 nm, and 100 nm Cu-Ni plates

The performance of Cu-Ni electrodes of varying thicknesses for electrochemical NO_3^- reduction and product formation (NO_2^-, NH_4^+, and gaseous compounds (GC)) with time is shown in Figure 4.

Figures 4A1,B1,C1 shows that the concentration of NO_3^- decreased with reaction time. The concentration of NO_2^-, NH_4^+, and GC increased with time for all electrode as seen from Figures 4A2,B2,C2 and Figures 4A3,B3,C3), respectively, while the concentration of gaseous compounds (GC) remained relatively stable (Figures 4A4,B4,C4). The thickness of the Cu film on the Ni plate does not appear to have a substantial effect on NO_3^- conversion under the conditions that were tested. This can be attributed to the use of sodium sulfate (Na_2SO_4), which was employed as the electrolyte in NO_3^- reduction experiments. Because, it closely replicates the neutral, unbuffered environment of real-world NO_3^- contaminated water (Costa et al., 2024). However, the presence of SO_4^{2-} ions in the solution may hinder the adsorption of NO_3^- on the Cu active sites (De Vooys et al., 2000). Moreover, high concentration of OH^- (aq) can cause a poisoning effect on the electrode causing a decrease in NO_3^- reduction (Wang et al., 2007) as can be seen from Figure 5.

Figure 5 depicts the changes in the pH of the anolyte and catholyte solutions. Initially, the pH range of both solutions was approximately 5.5–6.5, for all experiments carried out with 25, 50, and 100 nm Cu-Ni electrodes. During the first hour of the experiment, the pH of the anolyte suddenly dropped and became acidic, while the pH of the catholyte rose rapidly and became alkaline. Thereafter, the pH of both solutions changed very slowly until the end of the experiment, indicating that NO_3^- reduction on the Cu-Ni electrode was possible in alkaline conditions as well (Beltrame et al., 2020). This behavior is attributed to the reactions

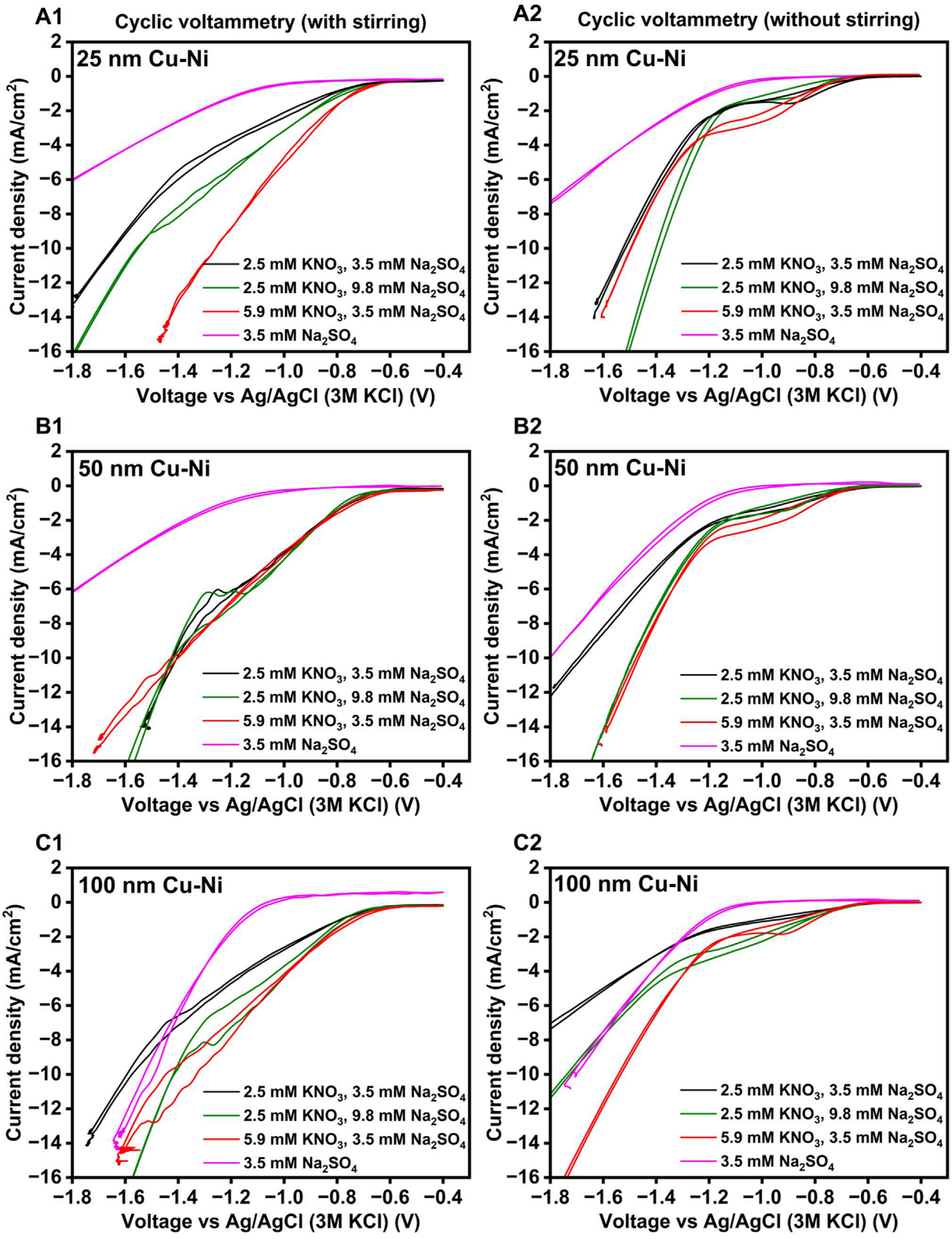

FIGURE 3
Cyclic voltammetry was recorded for Cu-Ni electrodes with varying Cu film thicknesses: **(A1,A2)** at 25 nm, **(B1,B2)** at 50 nm, and **(C1,C2)** at 100 nm, under N_2 sparging and with different concentrations of KNO_3 and Na_2SO_4 electrolyte. Additionally, **(A1,B1, and C1)** represent cyclic voltammetry measurements with stirring at 500 rpm, while **(A2,B2, and C2)** represent measurements without stirring, with a scan rate of 1 mV/s and an initial pH of 6.5.

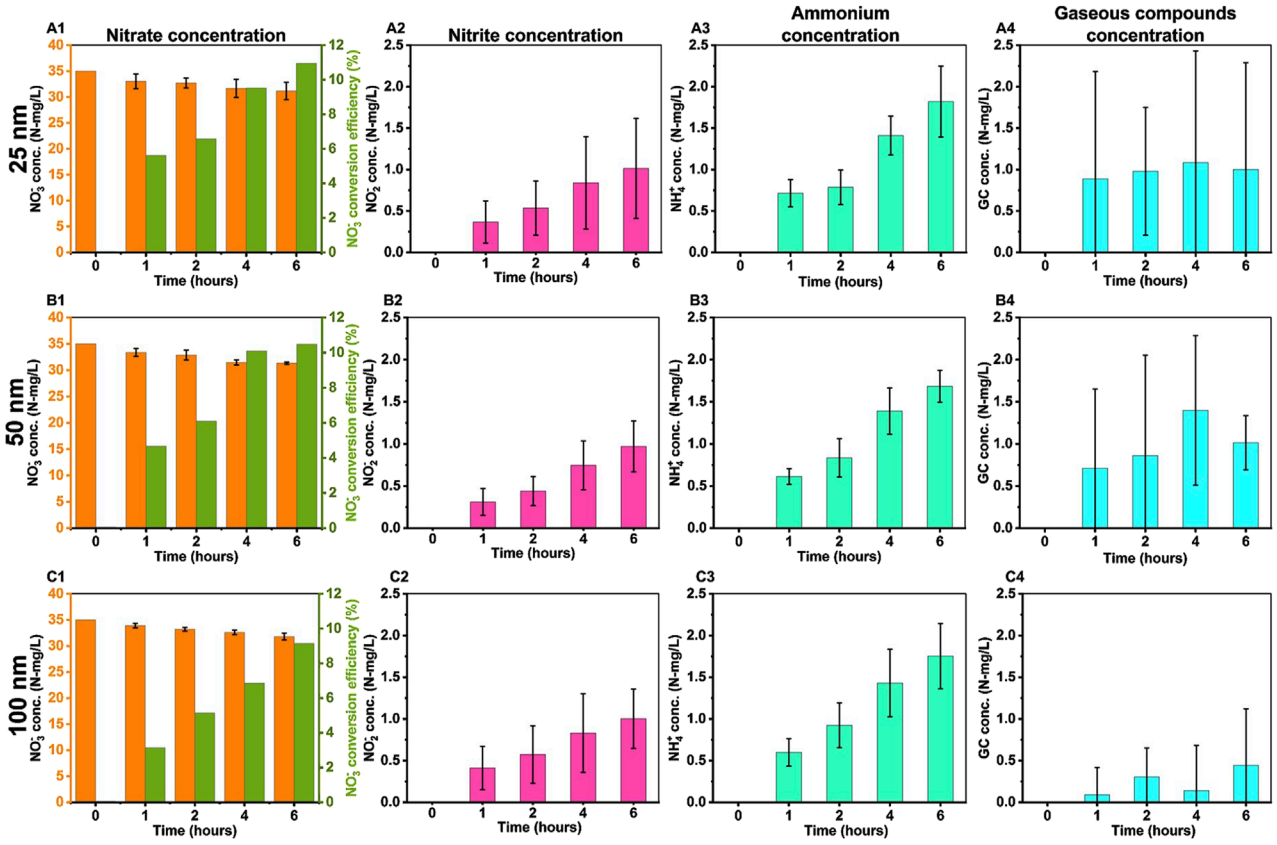

FIGURE 4
The concentrations (N-mg/L) of nitrate reduction reaction products were measured using a Cu-Ni electrode with varying Cu film thicknesses: **(A1–A4)** at 25 nm, **(B1–B4)** at 50 nm, and **(C1–C4)** at 100 nm. The experimental conditions included 2.5 mM KNO_3, 3.5 mM Na_2SO_4, an uncontrolled pH starting at 6.5, an applied current of −8.5 mA, and a duration of 6 h. The notations **(A1,B1, and C1)**], **(A2,B2, and C2)**, **(A3,B3, and C3)**, and **(A4,B4, and C4)** correspond to the concentrations of NO_3^-, NO_2^-, NH_4^+, and GC, respectively.

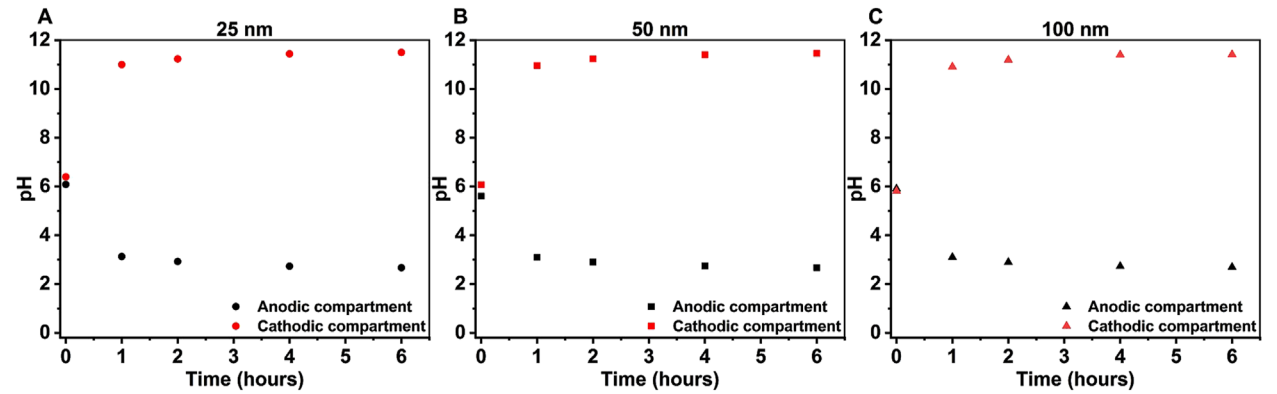

FIGURE 5
Changes in pH during NO_3^- reduction for **(A)** 25 nm Cu-Ni, **(B)** 50 nm Cu-Ni, and **(C)** 100 nm Cu-Ni at an applied current of −8.5 mA in 2.5 mM KNO_3 and 3.5 mM Na_2SO^4.

that occur at the electrodes where OH^- (aq) formation in the cathodic compartment (reactions [1]-[5]) increases the pH over time and H^+ (aq) formation in the anodic compartment where water electrolysis occurs decreases the pH according to Equation 9

$$\text{Reaction at anode: } H_2O \rightarrow \frac{1}{2}O_2 + 2H^+ + 2e^- \quad (9)$$

TABLE 2 NO_3RR conversion rate with respect to preparation technique of Cu coating on Ni.

Preparation technique	Ni structure	Surface area of working electrode (cm^2)	Initial pH	Electrolyte composition	Nitrate conversion rate	Ref
Electrochemical deposition	Ni foils (0.2 mm thick)	15	NA	45 mg/L NO_3^--N +0.1 M Na_2SO_4	29% after 48 h	Hou et al. (2018)
Electrodeless plating	Ni foam (sheet thickness = 2 mm)	80	12.5	50 mg/L NO_3^--N +0.1 M Na_2SO_4	For 4 h with Cu-Ni electrodes prepared using electrodeless Cu plating on Ni at different duration) a) Cu = 10% b) Cu/Ni/5 min = 60% c) Cu/Ni/10 min = 96% d) Cu/Ni/20 min = 92% e) Cu/Ni/40 min = 80% f) Cu/Ni/60 min = 50%	Shih et al. (2020)
Chemical deposition	Ni sponges	15	6.0–6.5	600 mg/L $NaNO_3$ + 1,400 mg/L Na_2SO_4	44% ± 5% after 6 h	Beltrame et al. (2020)
Potentiostatic deposition	Polycrystalline Ni electrode	0.03	NA	5 mM $NaNO_3$ + 0.1 M NaOH	Not mentioned	BADEA and BADEA (2003)
Physical vapor deposition	Ni plate	5.2	5.5–6.5	2.5 mM KNO_3 +3.5 mM Na_2SO_4	For 6 h with Cu-Ni electrode prepared using various thickness of Cu deposited on Ni by PVD a) Cu/Ni/25 nm = 10.9% b) Cu/Ni/50 nm = 10.5% c) Cu/Ni/100 nm = 10.0%	This study

The low NO_3^- reduction activity of Cu can be attributed to its unfavorable electronic state and the slow proton transfer at its surface, which is particularly significant in neutral or alkaline environment (Liu Z. et al., 2023). The NO_3^- reduction activity can be increased by alloying Cu with Ni, which transform the unfavorable electronic state into a favorable one, resulting in an increased production of atomic hydrogen. Additionally, the three-dimensional porous structure of the alloy enhances active sites, accelerates reaction kinetics, and boosts electrocatalytic activity (Ma et al., 2024). The Cu-Ni alloy also changes the adsorption energies of intermediates like NO_3^-, NO_2^-, and NH_2, improving efficiency, selectivity, and reducing toxic NO_2^- buildup (Li R. et al., 2023; Ma et al., 2024). Compared to monometallic Cu, the Cu-Ni alloy exhibits higher initial currents and reduced current decay over time, making it more effective for NO_3^- reduction (Wang et al., 2020). In acidic media, Cu-Ni alloy electrodes outperform pure Cu or Ni electrodes, minimizing undesired side reactions like hydrogen evolution, and offering superior corrosion resistance and catalytic performance, essential for the long-term stability and efficiency of the NO_3^- reduction process (Lou et al., 2024). The Cu-Ni alloy's ability to reduce energy barriers for intermediate steps is crucial for efficient NO_3^- reduction in water treatment applications, and it performs well across various NO_3^- concentrations and in simulated wastewater, demonstrating its robustness and broad applicability in NO_3^- reduction (Li R. et al., 2023; Wei J. et al., 2024). Here, it has been demonstrated that PVD can effectively be used to synthesize catalysts for NO_3^- reduction but that further optimization of electrodes by coating Cu coatings as thin films along with Ni addition must be done to reach higher conversion efficiency, conversion rates, selectivity and product concentration. Table 2 shows the NO_3^- conversion rate of Cu-coated Ni electrodes, prepared on different Ni structures using various coating techniques. It also shows the NO_3^- conversion rates for each study showing that these electrodes provides promising NO_3RR performance. As evidenced by Table 2 and from the literature (Meng et al., 2023), the conversion rate of NO_3^- is influenced by various factors, including the method

of catalyst preparation, the structure of the Ni substrate, the surface area of the electrode, the amount of NO_3^- used, initial pH and the duration of the experiments conducted. In this study, only pure Cu was deposited on the Ni plate using PVD and ca.10.5% efficiency has been achieved. Use of PVD technique for electrode preparation is still promising because it can deposit up to 750 k atoms/min, making it suitable for rapid coating deposition, resulting in uniform film deposition which is confirmed from SEM analysis also. The evaporation process in PVD results in lower absorbed gas within the film, contributing to coatings' purity and quality which is confirmed from Supplementary Figure S3 where the XPS of pristine 25 nm Cu-Ni electrode shows that no other metal impurities are present other than Cu, Ni, and oxygen. It is particularly versatile for industrial applications requiring thick films where surface morphology is not the primary quality requirement (Baptista et al., 2018).

4 Future work and scope

In future work, reaction mechanisms must be investigated further, e.g., by employing advanced techniques such as *in-situ* spectroscopic methods (e.g., FTIR, Raman) to identify the reaction intermediates and elucidate the rate-determining steps involved in NO_3^- reduction. Further, systematic studies must be conducted to comprehend the synergistic effects between Cu and Ni, including the role of interfacial properties and electronic interactions in enhancing catalytic activity, and utilize computational modelling techniques (e.g., DFT) to gain insights into the adsorption and reaction pathways of NO_3^- on the Cu-Ni surface (Wang Z. et al., 2021). Furthermore, rotating disk electrode experiments should be conducted on electrodes prepared using the PVD method to determine the kinetic current density and elucidate the electrocatalytic effect of Cu thin layers on Ni in the NO_3^- reduction reaction. The findings of this study, particularly the influence of Cu layer thickness on the NO_3RR performance, can inform the design of advanced electrodes for environmental remediation. Moreover, these electrodes could be employed in biosensors (Salazar et al., 2016), for energy storage as in supercapacitor (Madito et al., 2020), in microelectronic applications (Zhang et al., 2020), high-salt wastewater treatment (Tan et al., 2022), and in batteries (Pan et al., 2019; Liu et al., 2022; Lu J. et al., 2024). To further enhance the significance of this work, future studies should explore the durability and long-term performance of Cu-Ni electrodes under continuous operation and real-world conditions, investigate the synergistic effects of varying Cu deposition techniques, such as electrodeposition, alongside PVD, extend the approach to other electroactive species (e.g., NO_2^-, NH_3), to develop multi-functional electrocatalysts for broader environmental applications.

5 Conclusion

This study investigated the influence of the Cu layer thickness on NO_3^- electrochemical reduction using Cu-Ni composite electrodes produced by Physical Vapor Deposition (PVD). Scanning electron microscopy (SEM) and X-ray photoelectron spectroscopy (XPS) analyses confirmed the uniform distribution of thin Cu film on the Ni plate, with small pits which played a critical role in NO_3^- reduction and NH_4^+ selectivity. Similar NO_3^- conversion and product formation rates were obtained on all electrodes regardless of the thickness of the Cu layer. Based on the experimental results, it can be concluded that the NO_3^- removal efficiency with respect to electrode preparation techniques achieved by the PVD method is approximately 10% for varying thicknesses of Cu on Ni plate after 6 h, which is lower compared to other electrode preparation techniques. Furthermore, a decrease in current density was observed with an increase in the thickness of Cu on the Ni plate. Noting the importance of both Cu and Ni, present in a Cu-Ni alloy, it is essential to conduct further investigation in order to deposit pure thin Cu and Ni films combinedly on a Ni plate through PVD for efficient NO_3RR.

Data availability statement

The raw data supporting the conclusions of this article will be made available by the authors, without undue reservation.

Author contributions

SM: Conceptualization, Data curation, Funding acquisition, Investigation, Methodology, Visualization, and Writing – original draft. PG: Formal Analysis, Investigation, Software, and Writing – review and editing. PT: Resources, and Writing – review and editing. LJ: Conceptualization, Formal Analysis, Methodology, Supervision, and Writing – review and editing. SP: Conceptualization, Methodology, Supervision, and Writing – review and editing.

Funding

The author(s) declare that financial support was received for the research and/or publication of this article. This work was supported by the Ministry of Social Justice and Special Assistance Department, Government of Maharashtra, India.

Conflict of interest

The authors declare that the research was conducted in the absence of any commercial or financial relationships that could be construed as a potential conflict of interest.

The author(s) declared that they were an editorial board member of Frontiers, at the time of submission. This had no impact on the peer review process and the final decision.

Generative AI statement

The author(s) declare that no Generative AI was used in the creation of this manuscript.

Publisher's note

All claims expressed in this article are solely those of the authors and do not necessarily represent those of their affiliated organizations, or those of the publisher, the editors and the reviewers. Any product that may be evaluated in this article, or claim that may be made by its manufacturer, is not guaranteed or endorsed by the publisher.

Supplementary material

The Supplementary Material for this article can be found online at: https://www.frontiersin.org/articles/10.3389/fmats.2025.1527753/full#supplementary-material

References

Abascal, E., Gómez-Coma, L., Ortiz, I., and Ortiz, A. (2022). Global diagnosis of nitrate pollution in groundwater and review of removal technologies. *Sci. total Environ.* 810, 152233. doi:10.1016/j.scitotenv.2021.152233

Abba, S. I., Egbueri, J. C., Benaafi, M., Usman, J., Usman, A. G., and Aljundi, I. H. (2023). Fluoride and nitrate enrichment in coastal aquifers of the Eastern Province, Saudi Arabia: the influencing factors, toxicity, and human health risks. *Chemosphere* 336, 139083. doi:10.1016/j.chemosphere.2023.139083

Abdallah, R., Geneste, F., Labasque, T., Djelal, H., Fourcade, F., Amrane, A., et al. (2014). Selective and quantitative nitrate electroreduction to ammonium using a porous copper electrode in an electrochemical flow cell. *J. Electroanal. Chem.* 727, 148–153. doi:10.1016/j.jelechem.2014.06.016

Abdullah, S. S. (2017). Electrodeposition of nickel/copper multi-nanolayer by dual bath technique at ambient temperature. Available online at: https://www.semanticscholar.org/paper/Electrodeposition-of-nickel-copper-multi-nanolayer-Abdullah/0551b88b98f13fa978ea1e9e4062dd4d43d45c00 (Accessed February 26, 2025).

Abegunde, O. O., Akinlabi, E. T., Oladijo, O. P., Akinlabi, S., and Ude, A. U. (2019). Overview of thin film deposition techniques. *AIMS Mater. Sci.* 6, 174–199. doi:10.3934/matersci.2019.2.174

Ahn, J.-H., Choo, K.-H., and Park, H.-S. (2008). Reverse osmosis membrane treatment of acidic etchant wastewater: effect of neutralization and polyelectrolyte coating on nitrate removal. *J. Membr. Sci.* 310, 296–302. doi:10.1016/j.memsci.2007.11.010

Alam, M. M., Hasnat, M. A., Rashed, M. A., Uddin, S. M. N., Rahman, M. M., Amertharaj, S., et al. (2015). Nitrate detection activity of Cu particles deposited on pencil graphite by fast scan cyclic voltammetry. *J. Anal. Chem.* 70, 60–66. doi:10.1134/S1061934815010037

Badea, G. E. (2009). Electrocatalytic reduction of nitrate on copper electrode in alkaline solution. *Electrochimica Acta* 54, 996–1001. doi:10.1016/j.electacta.2008.08.003

Badea, G. E., and Badea, T. (2003). Nitrate reduction in alkaline solutions mediated by Cu and Cd underpotential deposition on Au and Ni substrates. *Rev. Roum. Chim.* 48, 843.

Bai, Z., Li, X., Ding, L., Qu, Y., and Chang, X. (2023). Artificial Cu-Ni catalyst towards highly efficient nitrate-to-ammonia conversion. *Sci. China Mat.* 66, 2329–2338. doi:10.1007/s40843-022-2392-8

Baptista, A., Silva, F. J. G., Porteiro, J., Míguez, J. L., Pinto, G., and Fernandes, L. (2018). On the physical vapour deposition (PVD): evolution of magnetron sputtering processes for industrial applications. *Procedia Manuf.* 17, 746–757. doi:10.1016/j.promfg.2018.10.125

Barrera, L., Silcox, R., Giammalvo, K., Brower, E., Isip, E., and Bala Chandran, R. (2023). Combined effects of concentration, pH, and polycrystalline copper surfaces on electrocatalytic nitrate-to-ammonia activity and selectivity. *ACS Catal.* 13, 4178–4192. doi:10.1021/acscatal.2c05136

Beltrame, T. F., Carvalho, D., Marder, L., Ulla, M. A., Marchesini, F. A., and Bernardes, A. M. (2020). Comparison of different electrode materials for the nitrate electrocatalytic reduction in a dual-chamber cell. *J. Environ. Chem. Eng.* 8, 104120. doi:10.1016/j.jece.2020.104120

Beltrame, T. F., Zoppas, F. M., Ferreira, J. Z., Marchesini, F. A., and Bernardes, A. M. (2021a). Nitrate reduction by electrochemical processes using copper electrode: evaluating operational parameters aiming low nitrite formation. *Water Sci. Technol.* 84, 200–215. doi:10.2166/wst.2021.215

Beltrame, T. F., Zoppas, F. M., Gomes, M. C., Ferreira, J. Z., Marchesini, F. A., and Bernardes, A. M. (2021b). Electrochemical nitrate reduction of brines: improving selectivity to N2 by the use of Pd/activated carbon fiber catalyst. *Chemosphere* 279, 130832. doi:10.1016/j.chemosphere.2021.130832

Bouzek, K., Paidar, M., Sadilkova, A., and Bergmann, H. (2001). Electrochemical reduction of nitrate in weakly alkaline solutions. *J. Appl. Electrochem.* 31, 1185–1193. doi:10.1023/a:1012755222981

Bu, X., Wei, R., Cai, Z., Quan, Q., Zhang, H., Wang, W., et al. (2021). More than physical support: the effect of nickel foam corrosion on electrocatalytic performance. *Appl. Surf. Sci.* 538, 147977. doi:10.1016/j.apsusc.2020.147977

Burke, L. D., and Sharna, R. (2007). Surface active state involvement in electrocatalytic reductions at copper in acid solution. *J. Appl. Electrochem* 37, 1119–1128. doi:10.1007/s10800-007-9370-9

Cattarin, S. (1992). Electrochemical reduction of nitrogen oxyanions in 1 M sodium hydroxide solutions at silver, copper and CuInSe2 electrodes. *J. Appl. Electrochem* 22, 1077–1081. doi:10.1007/BF01029588

Chen, J.-Q., Ye, X.-X., Zhou, D., and Chen, Y.-X. (2023). Roles of copper in nitrate reduction at copper-modified Ru/C catalysts. *J. Phys. Chem. C* 127, 2918–2928. doi:10.1021/acs.jpcc.2c07813

Chen, P.-Y., and Chang, Y.-T. (2012). Voltammetric study and electrodeposition of copper in 1-butyl-3- methylimidazolium salicylate ionic liquid. *Electrochimica Acta* 75, 339–346. doi:10.1016/j.electacta.2012.05.024

Chen, Y. X., Zhang, Y., Liu, H. Y., Sharma, K. R., and Chen, G. H. (2004). Hydrogen-based tubular catalytic membrane for removing nitrate from groundwater. *Environ. Technol.* 25, 227–234. doi:10.1080/09593330409355456

Cornet, A. J., Homborg, A. M., Anusuyadevi, P. R., 't Hoen-Velterop, L., and Mol, J. M. C. (2024). Unravelling corrosion degradation of aged aircraft components protected by chromate-based coatings. *Eng. Fail. Anal.* 159, 108070. doi:10.1016/j.engfailanal.2024.108070

Costa, G. F., Winkler, M., Mariano, T., Pinto, M. R., Messias, I., Souza, J. B., et al. (2024). Identifying the active site of Cu/Cu2O for electrocatalytic nitrate reduction reaction to ammonia. *Chem. Catal.* 4, 100850. doi:10.1016/j.checat.2023.100850

Couto, A. B., Baldan, M. R., and Ferreira, N. G. (2012). Copper photoelectrodeposition onto boron doped diamond electrodes at different doping level to enhance nitrate electroreduction. *MRS Proc.* 1395, 45–50. doi:10.1557/opl.2012.338

Couto, A. B., Oishi, S. S., Sardinha, A. F., and Ferreira, N. G. (2017). Electrocatalytic performance of three dimensional electrode Cu/reduced graphene oxide/carbon fiber for nitrate reduction. *ECS Trans.* 80, 1081–1087. doi:10.1149/08010.1081ecst

Couto, A. B., Santos, L. C. D., Matsushima, J. T., Baldan, M. R., and Ferreira, N. G. (2011). Hydrogen and oxygen plasma enhancement in the Cu electrodeposition and consolidation processes on BDD electrode applied to nitrate reduction. *Appl. Surf. Sci.* 257, 10141–10146. doi:10.1016/j.apsusc.2011.07.006

de Groot, M. T., and Koper, M. T. M. (2004). The influence of nitrate concentration and acidity on the electrocatalytic reduction of nitrate on platinum. *J. Electroanal. Chem.* 562, 81–94. doi:10.1016/j.jelechem.2003.08.011

Dejang, N., Klinbumrung, A., and Sirirak, R. (2025). Effective CuSO4 concentration on phase formation and optical characteristics of electrodeposited Ni-Cu alloy. *Trends Sci.* 22, 8897. doi:10.48048/tis.2025.8897

Della Rocca, C., Belgiorno, V., and Meriç, S. (2007). Overview of *in-situ* applicable nitrate removal processes. *Desalination* 204, 46–62. doi:10.1016/j.desal.2006.04.023

De Vooys, A. C. A., Van Santen, R. A., and Van Veen, J. A. R. (2000). Electrocatalytic reduction of NO-3 on palladium/copper electrodes. *J. Mol. Catal. A Chem.* 154, 203–215. doi:10.1016/S1381-1169(99)00375-1

Dima, G. E., De Vooys, A. C. A., and Koper, M. T. M. (2003). Electrocatalytic reduction of nitrate at low concentration on coinage and transition-metal electrodes in acid solutions. *J. Electroanal. Chem.* 554, 15–23. doi:10.1016/s0022-0728(02)01443-2

El Midaoui, A., Elhannouni,, F., Taky, M., Chay, L., Sahli, M. A. M., Echihabi, L., et al. (2002). Optimization of nitrate removal operation from ground water by electrodialysis. *Sep. Purif. Technol.* 29 (3), 235–244. doi:10.1016/S1383-5866(02)00092-8

Epron, F., Gauthard, F., and Barbier, J. (2002). Influence of oxidizing and reducing treatments on the metal-metal interactions and on the activity for nitrate reduction of a Pt-Cu bimetallic catalyst. *Appl. Catal. A General* 237, 253–261. doi:10.1016/S0926-860X(02)00331-9

Epron, F., Gauthard, F., Pinéda, C., and Barbier, J. (2001). Catalytic reduction of nitrate and nitrite on Pt-Cu/Al2O3 catalysts in aqueous solution: role of the interaction between copper and platinum in the reaction. *J. Catal.* 198, 309–318. doi:10.1006/jcat.2000.3138

Feng, A., Hu, Y., Yang, X., Lin, H., Wang, Q., Xu, J., et al. (2024). ZnO nanowire arrays decorated with Cu nanoparticles for high-efficiency nitrate to ammonia conversion. *ACS Catal.* 14, 5911–5923. doi:10.1021/acscatal.3c04398

Feng, Y., Liu, X., Yi, Z., Tan, H., Wang, L., Hou, F., et al. (2022). Ni-nanoparticle-modified Cu nanowires for enhanced electrocatalytic nitrate removal. *Surf. Innov.* 10, 402–410. doi:10.1680/jsuin.22.00040

Ganchev, M., Gergova, R., Terziyska, P., Popkirov, G., and Vitanov, P. (2021). Direct thermal evaporation of thin films copper (I) bromide. *Mater. Today Proc.* 37, A16–A20. doi:10.1016/j.matpr.2021.05.244

Gao, W., Gao, L., Li, D., Huang, K., Cui, L., Meng, J., et al. (2018). Removal of nitrate from water by the electrocatalytic denitrification on the Cu-Bi electrode. *J. Electroanal. Chem.* 817, 202–209. doi:10.1016/j.jelechem.2018.04.006

Gao, W., Gao, L., Meng, J., Li, D., Guan, Y., Cui, L., et al. (2019). Preparation of a novel Cu-Sn-Bi cathode and performance on nitrate electroreduction. *Water Sci. Technol.* 79, 198–206. doi:10.2166/wst.2019.049

Gonzalez-Gallardo, C. L., Morales-Hernández, J., Álvarez-Contreras, L., Arjona, N., and Guerra-Balcázar, M. (2024). Electrochemical detection of creatinine on Cu/carbon paper electrodes obtained by physical vapor deposition. *J. Appl. Electrochem.* 54, 115–126. doi:10.1007/s10800-023-01943-7

Goranova, D., Rashkov, R., Avdeev, G., and Tonchev, V. (2016). Electrodeposition of Ni–Cu alloys at high current densities: details of the elements distribution. *J. Mater Sci.* 51, 8663–8673. doi:10.1007/s10853-016-0126-y

Guo, J., Brimley, P., Liu, M. J., Corson, E. R., Muñoz, C., Smith, W. A., et al. (2023). Mass transport modifies the interfacial electrolyte to influence electrochemical nitrate reduction. *ACS Sustain. Chem. Eng.* 11, 7882–7893. doi:10.1021/acssuschemeng.3c01057

Guo, W., Zhang, K., Liang, Z., Zou, R., and Xu, Q. (2019). Electrochemical nitrogen fixation and utilization: theories, advanced catalyst materials and system design. *Chem. Soc. Rev.* 48, 5658–5716. doi:10.1039/C9CS00159J

Hao, D., Chen, Z., Figiela, M., Stepniak, I., Wei, W., and Ni, B.-J. (2021). Emerging alternative for artificial ammonia synthesis through catalytic nitrate reduction. *J. Mater. Sci. and Technol.* 77, 163–168. doi:10.1016/j.jmst.2020.10.056

Hasnat, M. A., Ben Aoun, S., Rahman, M. M., Asiri, A. M., and Mohamed, N. (2015). Lean Cu-immobilized Pt and Pd films/–H+ conducting membrane assemblies: relative electrocatalytic nitrate reduction activities. *J. Industrial Eng. Chem.* 28, 131–137. doi:10.1016/j.jiec.2015.02.008

He, L., Yao, F., Zhong, Y., Tan, C., Hou, K., Pi, Z., et al. (2022a). Achieving high-performance electrocatalytic reduction of nitrate by N-rich carbon-encapsulated Ni-Cu bimetallic nanoparticles supported nickel foam electrode. *J. Hazard. Mater.* 436, 129253. doi:10.1016/j.jhazmat.2022.129253

He, W., Zhang, J., Dieckhöfer, S., Varhade, S., Brix, A. C., Lielpetere, A., et al. (2022b). Splicing the active phases of copper/cobalt-based catalysts achieves high-rate tandem electroreduction of nitrate to ammonia. *Nat. Commun.* 13, 1129. doi:10.1038/s41467-022-28728-4

Hong, M., Wang, Q., Sun, J., and Wu, C. (2022). A highly active copper-nanoparticle-based nitrate reduction electrocatalyst prepared by *in situ* electrodeposition and annealing. *Sci. Total Environ.* 827, 154349. doi:10.1016/j.scitotenv.2022.154349

Hou, M., Pu, Y., Qi, W., Tang, Y., Wan, P., Yang, X. J., et al. (2018). Enhanced electrocatalytic reduction of aqueous nitrate by modified copper catalyst through electrochemical deposition and annealing treatment. *Chem. Eng. Commun.* 205, 706–715. doi:10.1080/00986445.2017.1413357

Hu, T., Wang, C., Wang, M., Li, C. M., and Guo, C. (2021). Theoretical insights into superior nitrate reduction to ammonia performance of copper catalysts. *ACS Catal.* 11, 14417–14427. doi:10.1021/acscatal.1c03666

Hwang, S. (2012). Nanocomposite monolayer of copper and lead on gold and its effect on nitrate electroreduction. *Int. J. Electrochem. Sci.* 7, 1820–1826. doi:10.1016/s1452-3981(23)13842-9

Hyusein, C., and Tsakova, V. (2023). Nitrate detection at Pd-Cu-modified carbon screen printed electrodes. *J. Electroanal. Chem.* 930, 117172. doi:10.1016/j.jelechem.2023.117172

Ince, R., Alper, F. M. P., Yukselici, M. H., Asikoglu, A., and Allahverdi, C. (2012). CdTe nanocrystals studied through *in-situ* electro-modulation spectroscopy, 75–76. doi:10.1109/OMEE.2012.6464793

Jia, X., Hou, D., Wang, L., O'Connor, D., and Luo, J. (2020). The development of groundwater research in the past 40 years: a burgeoning trend in groundwater depletion and sustainable management. *J. Hydrology* 587, 125006. doi:10.1016/j.jhydrol.2020.125006

Jilani, A., Abdel-Wahab, M. S., and Hammad, A. H. (2017). Advance deposition techniques for thin film and coating. *Mod. Technol. Creating Thin-film Syst. Coatings* 2, 137–149. doi:10.5772/65702

Jin, M., Liu, J., Zhang, X., Zhang, S., Li, W., Sun, D., et al. (2024). Heterostructure Cu3P–Ni2P/CP catalyst assembled membrane electrode for high-efficiency electrocatalytic nitrate to ammonia. *Nano Res.* 17, 4872–4881. doi:10.1007/s12274-024-6474-z

Johnston, S., Chebiam, R., Simka, H., Fischer, P., and Dubin, V. (2004). *Direct plating of Cu on ruthenium for sub-45nm technology node interconnects gapfill*, 539–544.

Kabiraz, M. K., Kim, J., Lee, H. J., Park, S., Lee, Y. W., and Choi, S.-I. (2024). Nickel nanoplates enclosed by (111) facets as durable oxygen evolution catalysts in anion exchange membrane water electrolyzers. *Adv. Funct. Mater.* 34, 2406175. doi:10.1002/adfm.202406175

Kang, X., Zuo, Q., Yuan, C., Chen, S., and Zhao, Y. (2013). Low stress TaN thin film development for Mems/Sensor electrode application. *J. Circuits, Syst. Comput.* 22, 1340017. doi:10.1142/S0218126613400173

Karamad, M., Goncalves, T. J., Jimenez-Villegas, S., Gates, I. D., and Siahrostami, S. (2023). Why copper catalyzes electrochemical reduction of nitrate to ammonia. *Faraday Discuss.* 243, 502–519. doi:10.1039/d2fd00145d

Knobeloch, L., Salna, B., Hogan, A., Postle, J., and Anderson, H. (2000). Blue babies and nitrate-contaminated well water. *Environ. health Perspect.* 108, 675–678. doi:10.1289/ehp.00108675

Kobune, M., Takizawa, D., Nojima, J., Otomo, R., and Kamiya, Y. (2020). Catalytic reduction of nitrate in water over alumina-supported nickel catalyst toward purification of polluted groundwater. *Catal. Today* 352, 204–211. doi:10.1016/j.cattod.2020.01.037

Lange, R., Maisonhaute, E., Robin, R., and Vivier, V. (2013). On the kinetics of the nitrate reduction in concentrated nitric acid. *Electrochem. Commun.* 29, 25–28. doi:10.1016/j.elecom.2013.01.005

Leaković, S., Mijatović, I., Cerjan-Stefanović, Š., and Hodžić, E. (2000). Nitrogen removal from fertilizer wastewater by ion exchange. *Water Res.* 34, 185–190. doi:10.1016/S0043-1354(99)00122-0

Lei, X., Liu, F., Li, M., Ma, X., Wang, X., and Zhang, H. (2018). Fabrication and characterization of a Cu-Pd-TNPs polymetallic nanoelectrode for electrochemically removing nitrate from groundwater. *Chemosphere* 212, 237–244. doi:10.1016/j.chemosphere.2018.08.082

Li, B., Pan, X., Zhang, D., Lee, D.-J., Al-Misned, F. A., and Mortuza, M. G. (2015). Anaerobic nitrate reduction with oxidation of Fe(II) by Citrobacter Freundii strain PXL1 – a potential candidate for simultaneous removal of as and nitrate from groundwater. *Ecol. Eng.* 77, 196–201. doi:10.1016/j.ecoleng.2015.01.027

Li, J., Gao, J., Feng, T., Zhang, H., Liu, D., Zhang, C., et al. (2021). Effect of supporting matrixes on performance of copper catalysts in electrochemical nitrate reduction to ammonia. *J. Power Sources* 511, 230463. doi:10.1016/j.jpowsour.2021.230463

Li, R., Zhao, D., Zhang, L., Dong, K., Li, Q., and Fan, G. (2023a). Electrodeposited copper–nickel nanoparticles as highly efficient electrocatalysts for nitrate reduction to ammonia. *Sustain. Energy Fuels* 7, 4417–4422. doi:10.1039/D3SE00901G

Li, X., Zhao, X., Lv, J., Jia, X., Zhou, S., Huang, Y., et al. (2023b). Self-supported porous copper oxide nanosheet arrays for efficient and selective electrochemical conversion of nitrate ions to nitrogen gas. *J. Mater. Sci. and Technol.* 137, 104–111. doi:10.1016/j.jmst.2022.06.054

Liang, X., Zhu, H., Yang, X., Xue, S., Liang, Z., Ren, X., et al. (2022). Recent advances in designing efficient electrocatalysts for electrochemical nitrate reduction to ammonia. *Small Struct.* 4, 2200202. doi:10.1002/sstr.202200202

Liang, Y., Zeng, Y., Tang, X., Xia, W., Song, B., Yao, F., et al. (2023). One-step synthesis of Cu(OH)2-Cu/Ni foam cathode for electrochemical reduction of nitrate. *Chem. Eng. J.* 451, 138936. doi:10.1016/j.cej.2022.138936

Lim, J., Chen, Y., Cullen, D. A., Lee, S. W., Senftle, T. P., and Hatzell, M. C. (2023). PdCu electrocatalysts for selective nitrate and nitrite reduction to nitrogen. *ACS Catal.* 13, 87–98. doi:10.1021/acscatal.2c04841

Lima, A. S., Salles, M. O., Ferreira, T. L., Paixão, T. R. L. C., and Bertotti, M. (2012). Scanning electrochemical microscopy investigation of nitrate reduction at activated copper cathodes in acidic medium. *Electrochimica Acta* 78, 446–451. doi:10.1016/j.electacta.2012.06.075

Lin, J.-X., Liu, X.-M., Cui, C.-W., Bai, C.-Y., Lu, Y.-M., Fan, F., et al. (2017). A review of thickness-induced evolutions of microstructure and superconducting performance of REBa2Cu3O7−δ coated conductor. *Adv. Manuf.* 5, 165–176. doi:10.1007/s40436-017-0173-x

Liu, B., and Zou, B.-X. (2014). Electrocatalytic sensing of nitrate at Cu nanosheets electrodeposited on WO3/polyaniline modified electrode. *Adv. Mater. Res.* 881 (883), 159–164. doi:10.4028/www.scientific.net/amr.881-883.159

Liu, J.-X., Richards, D., Singh, N., and Goldsmith, B. R. (2019). Activity and selectivity trends in electrocatalytic nitrate reduction on transition metals. *Acs Catal.* 9, 7052–7064. doi:10.1021/acscatal.9b02179

Liu, X., Duan, Y., Cheng, X.-T., Zhao, H.-L., Liu, Z., and Wang, Y.-Q. (2023a). Cu/NiO nanorods for efficiently promoting the electrochemical nitrate reduction to ammonia. *Dalton Trans.* 52, 17470–17476. doi:10.1039/D3DT03352J

Liu, Y., Chen, M., Zhao, X., Zhang, H., Zhao, Y., and Zhou, Y. (2023b). Unlocking the potential of sub-nanometer-scale copper via confinement engineering: a remarkable approach for electrochemical nitrate-to-ammonia conversion in wastewater treatment. *Chem. Eng. J.* 475, 146176. doi:10.1016/j.cej.2023.146176

Liu, Y., Peng, W., Zhang, J., Li, S., Hu, R., Yuan, B., et al. (2022). Tuning the electronic properties of NiO anode by *in-situ* introducing metallic Cu for high capacity and long life-span lithium-ion batteries. *J. Alloys Compd.* 918, 165693. doi:10.1016/j.jallcom.2022.165693

Liu, Z., Shen, F., Shi, L., Tong, Q., Tang, M., Li, Y., et al. (2023c). Electronic structure optimization and proton-transfer enhancement on titanium oxide-supported copper nanoparticles for enhanced nitrogen recycling from nitrate-contaminated water. *Environ. Sci. Technol.* 57, 10117–10126. doi:10.1021/acs.est.3c03431

Lockhart, K., King, A., and Harter, T. (2013). Identifying sources of groundwater nitrate contamination in a large alluvial groundwater basin with highly diversified intensive agricultural production. *J. Contam. hydrology* 151, 140–154. doi:10.1016/j.jconhyd.2013.05.008

Löffler, F., and Siewert, C. (2004). Homogeneous coatings inside cylinders. *Surf. Coatings Technol.* 177–178, 355–359. doi:10.1016/j.surfcoat.2003.09.026

Lou, Y.-Y., Zheng, Q.-Z., Zhou, S.-Y., Fang, J.-Y., Akdim, O., Ding, X.-Y., et al. (2024). Phase-dependent electrocatalytic nitrate reduction to ammonia on janus Cu@Ni tandem catalyst. *ACS Catal.* 14, 5098–5108. doi:10.1021/acscatal.4c00479

Lu, J., Lv, S., Park, H. S., and Chen, Q. (2024a). Electrocatalytically active and charged natural chalcopyrite for nitrate-contaminated wastewater purification extended to energy storage Zn-NO3– battery. *J. Hazard. Mater.* 477, 135287. doi:10.1016/j.jhazmat.2024.135287

Lu, T.-F., Hsu, K.-N., Hsu, C.-C., Hsu, C.-Y., and Wu, Y. S. (2024b). Effect of Cu film thickness on Cu bonding quality and bonding mechanism. *Materials* 17, 2150. doi:10.3390/ma17092150

Ma, Z., Wang, C., Yang, T., Wei, G., Huang, J., Liu, M., et al. (2024). A 3D porous P-doped Cu–Ni alloy for atomic H*enhanced electrocatalytic reduction of nitrate to ammonia. *J. Mat. Chem. A* 12, 7654–7662. doi:10.1039/D3TA08086B

Madito, M. J., Matshoba, K. S., Ochai-Ejeh, F. U., Mongwaketsi, N., Mtshali, C. B., Fabiane, M., et al. (2020). Nickel-copper graphene foam prepared by atmospheric pressure chemical vapour deposition for supercapacitor applications. *Surf. Coatings Technol.* 383, 125230. doi:10.1016/j.surfcoat.2019.125230

Mattarozzi, L., Cattarin, S., Comisso, N., Gerbasi, R., Guerriero, P., Musiani, M., et al. (2017). Electrodeposition of compact and porous Cu-Pd alloy layers and their application to nitrate reduction in alkali. *Electrochimica Acta* 230, 365–372. doi:10.1016/j.electacta.2017.02.012

Meng, S., Ling, Y., Yang, M., Zhao, X., Osman, A. I., Al-Muhtaseb, A. H., et al. (2023). Recent research progress of electrocatalytic reduction technology for nitrate wastewater: a review. *J. Environ. Chem. Eng.* 11, 109418. doi:10.1016/j.jece.2023.109418

Moffat, A. S. (1998). Global nitrogen overload problem grows critical. *Science* 279, 988–989. doi:10.1126/science.279.5353.988

Molodkina, E. B., Ehrenburg, M. R., Polukarov, Y. M., Danilov, A. I., Souza-Garcia, J., and Feliu, J. M. (2010). Electroreduction of nitrate ions on Pt(1 1 1) electrodes modified by copper adatoms. *Electrochimica Acta* 56, 154–165. doi:10.1016/j.electacta.2010.08.105

Morgan, K. A., Tang, T., Zeimpekis, I., Ravagli, A., Craig, C., Yao, J., et al. (2019). High-throughput physical vapour deposition flexible thermoelectric generators. *Sci. Rep.* 9, 4393. doi:10.1038/s41598-019-41000-y

Mubarak, A., and Hamzah, E. (2005). *Review of physical vapour deposition (PVD) techniques for hard coating*. Jurnal Mekanikal.

Nguyen, T. A. K., Huang, Y., Dang, N. M., Lin, C.-H., Chen, W.-C., Wang, Z.-Y., et al. (2024). Effect of sputtering power and thickness ratios on the materials properties of Cu–W and Cu–Cr bilayer thin films using high power impulse magnetron and DC magnetron sputtering. *J. Vac. Sci. and Technol. A* 42, 053410. doi:10.1116/6.0003795

Nobili, F., Dsoke, S., Mancini, M., and Marassi, R. (2009). Interfacial properties of copper-coated graphite electrodes: coating thickness dependence. *Fuel Cells* 9, 264–268. doi:10.1002/fuce.200800087

O'Sullivan, J., Burgess, S., and Rimmer, N. (2002). Metal lift-off using physical vapour deposition. *Microelectron. Eng.* 64, 473–478. doi:10.1016/s0167-9317(02)00823-7

Paidar, M., Roušar, I., and Bouzek, K. (1999). Electrochemical removal of nitrate ions in waste solutions after regeneration of ion exchange columns. *J. Appl. Electrochem.* 29, 611–617. doi:10.1023/A:1026423218899

Pan, Y., Zeng, W., Hu, R., Li, B., Wang, G., and Li, Q. (2019). Investigation of Cu doped flake-NiO as an anode material for lithium ion batteries. *RSC Adv.* 9, 35948–35956. doi:10.1039/c9ra05618a

Park, J. Y., and Yoo, Y. J. (2009). Biological nitrate removal in industrial wastewater treatment: which electron donor we can choose. *Appl. Microbiol. Biotechnol.* 82, 415–429. doi:10.1007/s00253-008-1799-1

Pérez-Gallent, E., Figueiredo, M. C., Katsounaros, I., and Koper, M. T. M. (2017). Electrocatalytic reduction of Nitrate on Copper single crystals in acidic and alkaline solutions. *Electrochimica Acta* 227, 77–84. doi:10.1016/j.electacta.2016.12.147

Raaif, M., and Mohamed, S. H. (2017). The effect of Cu on the properties of CdO/Cu/CdO multilayer films for transparent conductive electrode applications. *Appl. Phys. A Mater. Sci. Process.* 123, 441. doi:10.1007/s00339-017-1050-y

Rajmohan, K. S., and Chetty, R. (2014). Nitrate reduction at electrodeposited copper on copper cathode. *ECS Trans.* 59, 397–407. doi:10.1149/05901.0397ecst

Rajmohan, K. S., and Chetty, R. (2017). Enhanced nitrate reduction with copper phthalocyanine-coated carbon nanotubes in a solid polymer electrolyte reactor. *J. Appl. Electrochem* 47, 63–74. doi:10.1007/s10800-016-1020-7

Ramos, A., Miranda-Hernández, M., and González, I. (2001). Influence of chloride and nitrate anions on copper electrodeposition in ammonia media. *J. Electrochem. Soc.* 148, C315–C321. doi:10.1149/1.1357176

Reyter, D. (2014). "Electrochemical reduction of nitrate," in *Encyclopedia of applied electrochemistry*. Editors G. Kreysa, K. Ota, and R. F. Savinell (New York, NY: Springer), 585–593. doi:10.1007/978-1-4419-6996-5_135

Reyter, D., Chamoulaud, G., Bélanger, D., and Roué, L. (2006). Electrocatalytic reduction of nitrate on copper electrodes prepared by high-energy ball milling. *J. Electroanal. Chem.* 596, 13–24. doi:10.1016/j.jelechem.2006.06.012

Rezaei-Sameti, M., and Zarei, P. (2018). NBO, AIM, HOMO–LUMO and thermodynamic investigation of the nitrate ion adsorption on the surface of pristine, Al and Ga doped BNNTs: a DFT study. *Adsorption* 24, 757–767. doi:10.1007/s10450-018-9977-7

Ribeiro, M. C. E., Couto, A. B., Ferreira, N. G., and Baldan, M. R. (2014). Nitrate removal by electrolysis using Cu/BDD electrode cathode. *ECS Trans.* 58, 21–26. doi:10.1149/05819.0021ecst

Rossnagel, S. M. (2003). Thin film deposition with physical vapor deposition and related technologies. *J. Vac. Sci. and Technol. A* 21, S74–S87. doi:10.1116/1.1600450

Roy, C., Deschamps, J., Martin, M., Bertin, E., Reyter, D., Garbarino, S., et al. (2016). Identification of Cu surface active sites for a complete nitrate-to-nitrite conversion with nanostructured catalysts. *Appl. Catal. B Environ.* 187, 399–407. doi:10.1016/j.apcatb.2016.01.043

Salazar, P., Rico, V., and González-Elipe, A. R. (2016). Nickel-copper bilayer nanoporous electrode prepared by physical vapor deposition at oblique angles for the non-enzymatic determination of glucose. *Sensors Actuators, B Chem.* 226, 436–443. doi:10.1016/j.snb.2015.12.003

Salazar, P., Rico, V., Rodríguez-Amaro, R., Espinós, J. P., and González-Elipe, A. R. (2015). New copper wide range nanosensor electrode prepared by physical vapor deposition at oblique angles for the non-enzimatic determination of glucose. *Electrochimica Acta* 169, 195–201. doi:10.1016/j.electacta.2015.04.092

Sancho, M., Álvarez-Blanco, S., Kombo, G., and García-Fayos, B. (2016). Experimental determination of nanofiltration models: application to nitrate removal. *Desalination Water Treat.* 57, 22852–22859. doi:10.1080/19443994.2016.1173380

Savale, P. (2016). Physical vapor deposition (PVD) methods for synthesis of thin films: a comparative study. *Arch. Appl. Sci. Res.* 8, 1–8.

Shah, A., Izman, S., Ismail, S. N. F., Ayu, M., Daud, H., and Abdul-Kadir, M. (2018). Physical Vapour Deposition on corrosion resistance: a review. *ARPN J. Eng. Appl. Sci.* 13, 3515–3523.

Shen, J., He, R., Han, W., Sun, X., Li, J., and Wang, L. (2009). Biological denitrification of high-nitrate wastewater in a modified anoxic/oxic-membrane bioreactor (A/O-MBR). *J. Hazard. Mater.* 172, 595–600. doi:10.1016/j.jhazmat.2009.07.045

Shih, Y.-J., Wu, Z.-L., Huang, Y.-H., and Huang, C.-P. (2020). Electrochemical nitrate reduction as affected by the crystal morphology and facet of copper nanoparticles supported on nickel foam electrodes (Cu/Ni). *Chem. Eng. J.* 383, 123157. doi:10.1016/j.cej.2019.123157

Smiljanić, M., Panić, S., Bele, M., Ruiz-Zepeda, F., Pavko, L., Gašparič, L., et al. (2022). Improving the HER activity and stability of Pt nanoparticles by titanium oxynitride support. *ACS Catal.* 12, 13021–13033. doi:10.1021/acscatal.2c03214

Sun, H.-T., Wang, X.-P., Kou, Z.-Q., Wang, L.-J., Wang, J.-Y., and Sun, Y.-Q. (2015). Optimization of TiO2/Cu/TiO2 multilayers as a transparent composite electrode deposited by electron-beam evaporation at room temperature. *Chin. Phys. B* 24, 047701. doi:10.1088/1674-1056/24/4/047701

Takahashi, T. (1998). Physical vapor deposition. *Ultraclean Surf. Process. Silicon Wafers Secrets VLSI Manuf.*, 352–360. doi:10.1007/978-3-662-03535-1_25

Tan, X., Wang, X., Zhou, T., Chen, T., Liu, Y., Ma, C., et al. (2022). Preparation of three dimensional bimetallic Cu–Ni/NiF electrodes for efficient electrochemical removal of nitrate nitrogen. *Chemosphere* 295, 133929. doi:10.1016/j.chemosphere.2022.133929

Tomer, M. D., Porter, S. A., James, D. E., Boomer, K. M., Kostel, J. A., and McLellan, E. (2013). Combining precision conservation technologies into a flexible framework to facilitate agricultural watershed planning. *J. Soil Water Conservation* 68, 113A–120A. doi:10.2489/jswc.68.5.113a

Varapragasam, S. J. P., Andriolo, J. M., Skinner, J. L., and Grumstrup, E. M. (2021). Photocatalytic reduction of aqueous nitrate with hybrid Ag/g-C3N4 under ultraviolet and visible light. *ACS Omega* 6, 34850–34856. doi:10.1021/acsomega.1c05523

Wang, C., Liu, J.-M., Wang, Y.-H., and Lu, X.-Y. (2023a). Study on the electrochemical reduction of nitrate using a modified Cu-Pd bimetallic electrode. *Zhongguo Huanjing Kexue/China Environ. Sci.* 43, 5196–5207.

Wang, H., Huang, J., Cai, J., Wei, Y., Cao, A., Liu, B., et al. (2023b). *In situ*/Operando methods for understanding electrocatalytic nitrate reduction reaction. *Small Methods* 7, 2300169. doi:10.1002/smtd.202300169

Wang, J., Zhang, Z., and Ding, S. (2022). Cu supported on the graphene oxide modified graphite felt electrode for highly efficient nitrate electroreduction. *J. Environ. Chem. Eng.* 10, 108092. doi:10.1016/j.jece.2022.108092

Wang, Y., Qu, J., and Liu, H. (2007). Effect of liquid property on adsorption and catalytic reduction of nitrate over hydrotalcite-supported Pd-Cu catalyst. *J. Mol. Catal. A Chem.* 272, 31–37. doi:10.1016/j.molcata.2007.02.028

Wang, Y., Wang, C., Li, M., Yu, Y., and Zhang, B. (2021a). Nitrate electroreduction: mechanism insight, *in situ* characterization, performance evaluation, and challenges. *Chem. Soc. Rev.* 50, 6720–6733. doi:10.1039/D1CS00116G

Wang, Y., Xu, A., Wang, Z., Huang, L., Li, J., Li, F., et al. (2020). Enhanced nitrate-to-ammonia activity on copper–nickel alloys via tuning of intermediate adsorption. *J. Am. Chem. Soc.* 142, 5702–5708. doi:10.1021/jacs.9b13347

Wang, Z., Richards, D., and Singh, N. (2021b). Recent discoveries in the reaction mechanism of heterogeneous electrocatalytic nitrate reduction. *Catal. Sci. Technol.* 11, 705–725. doi:10.1039/D0CY02025G

Wei, J., Li, Y., Lin, H., Lu, X., Zhou, C., and Li, Y. (2024a). Copper-based electro-catalytic nitrate reduction to ammonia from water: mechanism, preparation, and research directions. *Environ. Sci. Ecotechnology* 20, 100383. doi:10.1016/j.ese.2023.100383

Wei, M., Li, S., Wang, X., Zuo, G., Wang, H., Meng, X., et al. (2024b). A perspective on Cu-based electrocatalysts for nitrate reduction for ammonia synthesis. *Adv. Energy Sustain. Res.* 5, 2300173. doi:10.1002/aesr.202300173

Welch, C. M., Hyde, M. E., Banks, C. E., and Compton, R. G. (2005). The detection of nitrate using *in-situ* copper nanoparticle deposition at a boron doped diamond electrode. *Anal. Sci.* 21, 1421–1430. doi:10.2116/analsci.21.1421

Wu, L., Ko, E., Dulkin, A., Park, K. J., Fields, S., Leeser, K., et al. (2010). Flux and energy analysis of species in hollow cathode magnetron ionized physical vapor deposition of copper. *Rev. Sci. Instrum.* 81, 123502. doi:10.1063/1.3504371

Xu, H., Chen, J., Zhang, Z., Hung, C.-T., Yang, J., and Li, W. (2023). *In situ* confinement of ultrasmall metal nanoparticles in short mesochannels for durable electrocatalytic nitrate reduction with high efficiency and selectivity. *Adv. Mater.* 35, 2207522. doi:10.1002/adma.202207522

Yang, S., Wang, X., Song, Z., Liu, C., Li, Z., Wang, J., et al. (2022). Efficient electrocatalytic nitrate reduction in neutral medium by Cu/CoP/NF composite cathode coupled with Ir-Ru/Ti anode. *Chemosphere* 307, 136132. doi:10.1016/j.chemosphere.2022.136132

Yanguas-Gil, A., and Yanguas-Gil, A. (2017). "Physical and chemical vapor deposition techniques," in *Growth and transport in nanostructured materials: reactive transport in PVD, CVD, and ALD*, 19–37.

Yao, X., Yu, B., Xue, Y., Ran, X., Zuo, J., and Qiu, K. (2021). Selective conversion of nitrate to nitrogen by CuNi alloys embedded mesoporous carbon with breakpoint chlorination. *J. Water Process Eng.* 42, 102174. doi:10.1016/j.jwpe.2021.102174

Yin, D., Liu, Y., Song, P., Chen, P., Liu, X., Cai, L., et al. (2019). *In situ* growth of copper/reduced graphene oxide on graphite surfaces for the electrocatalytic reduction of nitrate. *Electrochimica Acta* 324, 134846. doi:10.1016/j.electacta.2019.134846

Yue, X., Wang, Y., Zhao, Y., Xiang, H., Shu, S., Zhang, P., et al. (2024). A novel self-supported catalytic electrode preparation method: synthesizing and printing Cu-based nanoparticles on nickel foam by cold plasma jet. *Appl. Surf. Sci.* 662, 160079. doi:10.1016/j.apsusc.2024.160079

Zhang, H., Wang, S., Tian, Y., Liu, Y., Wen, J., Huang, Y., et al. (2020). Electrodeposition fabrication of Cu@Ni core shell nanowire network for highly stable transparent conductive films. *Chem. Eng. J.* 390, 124495. doi:10.1016/j.cej.2020.124495

Zhang, X., Ma, G., Shui, L., Zhou, G., and Wang, X. (2022). Ni3N nanoparticles on porous nitrogen-doped carbon nanorods for nitrate electroreduction. *Chem. Eng. J.* 430, 132666. doi:10.1016/j.cej.2021.132666

Zhao, X., Geng, Q., Dong, F., Zhao, K., Chen, S., Yu, H., et al. (2023). Boosting the selectivity and efficiency of nitrate reduction to ammonia with a single-atom Cu electrocatalyst. *Chem. Eng. J.* 466, 143314. doi:10.1016/j.cej.2023.143314

Zhao, Y., Liu, Y., Zhang, Z., Mo, Z., Wang, C., and Gao, S. (2022). Flower-like open-structured polycrystalline copper with synergistic multi-crystal plane for efficient electrocatalytic reduction of nitrate to ammonia. *Nano Energy* 97, 107124. doi:10.1016/j.nanoen.2022.107124

Zurita, N., and Garcia, S. (2022). Influence of supporting electrolyte on electrochemical formation of copper nanoparticles and their electrocatalytic properties. *J. Electrochem. Sci. Eng.* 12, 253–264. doi:10.5599/jese.1077

Zurita, N., and García, S. G. (2023). Comparative study of electrodeposited copper nanoparticles on different substrates for their use in the reduction of nitrate ions. *Results Eng.* 17, 100800. doi:10.1016/j.rineng.2022.100800